Published in final edited form as:
J Immunol. 2014 November 1; 193(9): 4712–4721. doi:10.4049/jimmunol.1400202.

Dual role of the leukocyte integrin $\alpha_M\beta_2$ in angiogenesis

Dmitry A. Soloviev[*], **Stanley L. Hazen**[‡], **Dorota Szpak**[*], **Kamila M. Bledzka**[*], **Christie M. Ballantyne**[†], **Edward F. Plow**[*], and **Elzbieta Pluskota**[*]

[*]Joseph J. Jacobs Center for Thrombosis and Vascular Biology, Department of Molecular Cardiology, Cleveland Clinic, Cleveland, OH

[†]Baylor College of Medicine and Methodist DeBakey Heart and Vascular Center, Houston, TX

[‡]Department of Molecular and Cellular Medicine, Cleveland Clinic, Cleveland, OH

Abstract

Neutrophils (PMN) and macrophages are crucial contributors to neovascularization serving as a source of chemokines, growth factors and proteases. $\alpha_M\beta_2$(CD11b/CD18) and $\alpha_L\beta_2$(CD11a/CD18) are expressed prominently and have been implicated in various responses of these cell types. Thus, we investigated the role of these β_2 integrins in angiogenesis. Angiogenesis was analyzed in wild-type (WT), α_M-knockout ($\alpha_M^{-/-}$) and α_L-deficient ($\alpha_L^{-/-}$) mice using B16F10 melanoma, RM1 prostate cancer and matrigel implants. In all models, vascular area was decreased by 50–70% in $\alpha_M^{-/-}$ mice resulting in stunted tumor growth as compared to WT mice. In contrast, α_L deficiency did not impair angiogenesis and tumor growth. The neovessels in $\alpha_M^{-/-}$ mice were leaky and immature as they lacked smooth muscle cell and pericytes. Defective angiogenesis in the $\alpha_M^{-/-}$ mice was associated with attenuated neutrophil (PMN) and macrophage recruitment into tumors. In contrast to WT or the $\alpha_L^{-/-}$ leukocytes, the $\alpha_M^{-/-}$ myeloid cells showed impaired plasmin (Plm)-dependent ECM invasion, resulting from 50–75% decrease in plasminogen (Plg) binding and pericellular Plm activity. Surface plasmon resonance verified direct interaction of the α_MI-domain, the major ligand binding site in the β_2 integrins, with Plg. However, the α_LI-domain failed to bind Plg. Also, endothelial cells failed to form tubes in the presence of conditioned medium collected from TNF-α-stimulated PMNs derived from the $\alpha^{M-/-}$ mice due to severely impaired degranulation and secretion of VEGF. Thus, $\alpha_M\beta_2$ plays a dual role in angiogenesis, supporting not only Plm-dependent recruitment of myeloid cells to angiogenic niches, but also secretion of VEGF by these cells.

Introduction

Bone marrow derived myeloid cells, particularly neutrophils (PMNs) and macrophages, are key regulators of tumor progression and metastasis. One of the major tumor promoting functions of these cells is their facilitation of angiogenesis (reviewed in (1, 2)). PMNs and

[*]To whom correspondence should be addressed: Elzbieta Pluskota, Ph.D., Department of Molecular Cardiology, NB50, Lerner Research Institute, Cleveland Clinic, 9500 Euclid Avenue, Cleveland, OH, 44195, Phone 216-445-8211, Fax 216-445-8204, pluskote@ccf.org.

Disclosures
The authors have no financial conflicts of interest.

macrophages contribute to angiogenesis via a variety of well-established mechanisms. One example is their capacity to produce and secrete a variety of pro-angiogenic factors such as VEGF-A, FGF, IL-8, IL-10, CXCL1/GRO and COX-2 (3, 4). In addition, PMNs and macrophages are a rich source of numerous proteases including neutrophil elastase, cathepsin G and several metalloproteinases, which are crucial not only for ECM degradation and remodeling, but also regulate bioavailability of various proangiogenic stimuli (5), all requisite events in angiogenesis (reviewed in (4, 6–8)). In addition, both PMNs and macrophages secrete urokinase-type plasminogen activator (uPA), which converts plasminogen (Plg) to plasmin (Plm). There are diverse Plg receptors on leukocyte surface (reviewed in (9)) and bound Plm facilitates leukocyte migration/invasion by directly degrading ECM, and encourages leukocyte recruitment in a variety of in vivo models of inflammation (10–12).

$\alpha_M\beta_2$ (CD11b/CD18) and $\alpha_L\beta_2$ (CD11a/CD18), two the most broadly studied members of the β_2 integrin subfamily, are particularly enriched in PMNs and macrophages, where they regulate diverse cell functions, including migration, adhesion, the respiratory burst and cytokine production (13). In addition, we have previously demonstrated that $\alpha_M\beta_2$ enhances uPA-dependent Plg activation on the PMN surface (14, 15), which has the potential to influence their recruitment to inflammatory/angiogenic sites *in vivo*. Based on these observations, we hypothesized that $\alpha_M\beta_2$ and $\alpha_L\beta_2$, as key regulators of leukocyte functions, might be implicated in angiogenesis. Here, we used $\alpha_M^{-/-}$ and $\alpha_L^{-/-}$ mice and 3 distinct *in vivo* angiogenesis models to show that $\alpha_M\beta_2$, but not $\alpha_L\beta_2$, is a critical contributor to angiogenesis. This function of $\alpha_M\beta_2$ is mediated by two distinct mechanisms: 1) support of Plm-dependent PMN/macrophage recruitment to angiogenic niches; and 2) enhancement of leukocyte production and secretion of the primary angiogenic growth factor, VEGF-A.

Materials and Methods

Materials

Mouse VEGF165 and KC were from Biosource International (Camarillo, CA), heparin was from Sigma (St. Louis, MO), biotin-conjugated anti-mouse CD31 mAb was from BD Pharmigen (San Jose, CA), rabbit anti-Smooth Muscle Actin (SMA, Abcam, Cambridge, MA), rabbit anti-NG2 (Millipore, Temecula, CA), rabbit anti-mouse laminin (Serotec, Oxford, UK), goat anti-Fibrin II (Accurate Chemical, Westbury, NY), purified or FITC-labeled rat anti-Ly6G, clone 1A8, specific for mouse PMNs were from BD Pharmigen (San Jose, CA), anti-mouse macrophages/monocytes mAb (MOMA-2) was from Chemicon (Temecula, CA), rat LEAF TM purified anti-mouse α_M integrin (clone M1/70) was from Biolegend (San Diego, CA). Glu-Plg was isolated from normal human plasma by affinity chromatography on lysine-Sepharose followed by gel filtration. Growth Factor-reduced Matrigel matrix was from BD Bioscience (San Diego, CA). Murine recombinant TNFα was from R&D Systems, cycloheximide and pentoxifylline were from Sigma.

Mice

The $\alpha_M^{-/-}$ mice were generated as previously described (16), and $\alpha_L^{-/-}$ mice were purchased from the Jackson Laboratory. Both strains were backcrossed for 12 generations

into a C57BL/J6 background. The study was conducted under protocols approved by the IACUC of the Cleveland Clinic.

Angiogenesis models in vivo

8–12 week-old mice were injected subcutaneously with 10^6 murine B16F10 melanoma or RM1 prostate cancer cells. Tumors were collected 8–14 days after injection and were weighted, photographed and processed for immunohistochemical staining. EC were identified using a biotinylated mouse CD31 mAb, Smooth Muscle Cells with anti-SMA Ab, pericytes with anti-NG2 Ab, fibrin with anti-Fibrin II Ab, basement membrane with anti-laminin Ab, PMNs with rat anti-Ly6G (clone 1A8) and monocytes/macrophages with MOMA-2 mAbs. Stained sections were analyzed using fluorescent imaging microscopy (Leica, Germany) and ImagePro Plus Capture and Analysis software (Media Cybernetics). CD31, fibrin, Ly6G- or MOMA2-positive area was quantified in 5–10 independent fields. The average area per field was determined from duplicate measurements of each of the fields analyzed. Matrigel plug assay has been performed as described (17). Mice were injected with 500μl of growth factor-reduced Matrigel was mixed at 4°C with heparin (26U/ml) alone or with KC (Keratinocyte-derived cytokine) (500ng/ml) or VEGF 165 (100ng/ml) (R&D Systems). Matrigel plugs were harvested 8 days after injection, snap-frozen and 8 μm sections were processed for immunohistochemical analyses as described above. In α_M integrin blocking experiments, WT mice were injected intravenously with rat LEAF™ anti-mouse α_M integrin (clone M1/70) (Biolegend, San Diego, CA) or isotype matched normal rat IgG_{2b} (3.5 mg/kg), 4h before and then 2, 4 and 6 days after Matrigel-KC implantation. The Matrigel plugs were collected 8 days after injection, sectioned and stained with anti-CD31 to examine vascular formation.

Bone marrow transplantation

Two months old recipient mice were lethally X-irradiated with a total dose of 9Gy and reconstituted with intravenous injection of 10^7 BM cells isolated from the femurs of donor mice. Mice were used 6–8 weeks after BMT. Engraftment efficiency was examined 6 weeks after BMT in chimeric $\alpha_M^{-/-} \rightarrow$ WT and WT $\rightarrow \alpha_M^{-/-}$ mice using WT and $\alpha_M^{-/-}$ mice, which did not undergo BMT as controls. Single cell suspensions from spleens and thymuses from these mice were prepared and percentages of individual leukocyte subsets were measured by flow cytometry using FITC-labeled Abs to cell specific markers (Ly-6G for PMN, F4/80 for macrophages, CD19 for B lymphocytes, CD3 for T lymphocytes) and FITC-labeled isotype-matched Abs as controls.

Plg binding to α_M and α_L-I domains

GST-fused α_MI and α_LI domains were purified by glutathione chromatography. Real-time protein-protein interactions were analyzed using a Biacore 3000 instrument (BIAcore AB). Plg was immobilized on CM5 biosensor chips by amine coupling. Experiments were performed at 22°C in 10mM HEPES buffer, pH 7.4, containing 150mM NaCl and 0.005% surfactant P20 (flow rate, 25μL/minute). Surface plasmon resonance (SPR) sensograms were obtained by injecting various concentrations of GST-tagged α_MI or α_LI domain over immobilized Plg and reference flow cells. Surfaces were regenerated by 30s pulses of 10 mM NaOH. Association/dissociation curves were determined after the subtraction of the

reference surface values and buffer binding at 6 selected concentrations. Sensograms were analyzed using BIAevaluation software (version 4.01; GE Healthcare).

PMN and macrophage isolation

Mouse PMN for use in MAEC tube formation and Plg activation assays (see below), were isolated from blood drawn from hearts of anesthetized animals into sterile acid-citrate-dextrose (1:7 volume 145mM sodium citrate, pH 4.6, and 2% dextrose). Blood was transferred to 1.25% dextran T500 solution (1:9) to sediment erythrocytes for 30 min at RT (14, 18). Leukocyte-rich supernatants were washed with PBS once, and PMNs were isolated by magnetic positive selection using mouse anti-Ly6G MicroBead Isolation Kit (Miltenyi Biotec, Auburn, CA) according to manufacturer's instructions. Eluted cells were 98% granulocytes, of which more than 96% were neutrophils and 1–2% were eosinophils. Contaminating lymphocytes and monocytes were less than 2% as determined by Wright staining. PMN viability was >98% as determined by trypan blue staining. The PMN yield was usually ~0.5×10^6 per mouse, and blood pooled from 10–15 mice was used. For Plg activation assays lymphocytes and monocytes were collected from buffy coats, and washed twice with the HBSS buffer. Leukocytes were obtained from blood pooled from 7–10 mice. For matrix invasion and Plg binding assays, macrophages and PMN were isolated from peritoneal lavages, PMN at 6h and macrophages at 72h after intraperitoneal thioglycolate injection, when their recruitment was at highest levels for each cell type (10). PMNs constitute 92% and macrophages 90% of all cells in the 6h and 72h peritoneal lavages, respectively. PMN and macrophages harvested from lavages are referred to as peritoneal PMN or peritoneal macrophages in the manuscript to distinguish them from blood cells.

Matrix Invasion Assays ex Vivo

Prechilled tissue culture inserts with porous (8μm pore size) polyester membrane (Costar, Corning, NY) were coated with 50μl/insert of Matrigel (0.5mg/ml) overnight at 4°C until dry. Next, matrices were rehydrated with 600μL DMEM F-12 for 1h. Peritoneal PMNs or macrophages were suspended in serum-free DMEM F-12 medium (Gibco, Carlsbad, CA), and added to matrix-coated inserts (1×10^5/insert), which were placed in a 24-well plate containing serum-free DMEM F-12 supplemented with or without 100ng/ml KC. Plg (90μg/ml) was added to appropriate inserts, and cells were incubated for 18h at 37°C. Assays were stopped by removing the inserts and wiping the inside with a cotton swab to remove non-migrated cells. The migrated cells were quantified using the Cyquant Cell Proliferation Kit (Molecular Probes, Eugene, OR) according to manufacturer's instructions.

Plg Activation on the Leukocyte Surface

Peripheral blood PMNs or lymphocyte/monocyte mixtures were incubated with KC (100ng/ml) for 1h at 37°C in the presence of 25nM sc-uPA in 10mM Tris-Cl buffer, pH 7.4, containing 0.14mM NaCl, 0.1%BSA, 1mM $CaCl_2$ and 1mM $MgCl_2$. The cells were washed three times, and 50μl of the cell suspension (1×10^6cells/well) were added to each well of the microtiter plates. Peritoneal macrophages, which had not been incubated with KC or sc-uPA, were also added to the plates. Then, 100μl of a Glu-Plg (1μM) and Plm-specific fluorescent substrate H-D-Val-Leu-Lys-7-amido-4-methylcoumarin (2mM) mixture was

added, and Plm formation was monitored over 45min at 37°C at α_{em}=370nm and α_{ex}=470nm using a fluorescence plate reader (SpectraMax GeminiXS, Molecular Devices).

Regulation of VEGF by PMNs

Peripheral blood WT, $\alpha_M^{-/-}$ or $\alpha_L^{-/-}$ PMNs were incubated in 24-well tissue culture plates (Costar) (3×10^6 cells/well) in 250 μl of DMEM F-12 medium in the absence or presence of TNFα (20ng/ml) for 2h at 37°C. The inhibitors of protein synthesis (cycloheximide-10μg/ml) or PMN degranulation (pentoxifylline, 3,7-dimethyl-1-(5-oxohexyl)-xantine-300 μM) were added to PMNs 60 min before addition of TNFα. Supernatants were collected, centrifuged at 1500 rpm in a Beckman GS-6 centrifuge for 10 min and VEGF was measured using mouse VEGF Quantikine Elisa Kit (R&D Systems). In parallel, lactoferrin concentration was measured in PMN supernatants using mouse Lactoferrin LTF/LF Elisa Kit (Cusabio).

Quantitative Real Time PCR

Total RNA was isolated from peripheral blood mouse PMNs, either resting or stimulated with TNFα (20ng/ml) for 2h at 37 °C, and from WT and $\alpha_M^{-/-}$ mouse $CD117^+$ bone marrow progenitor cells with Trizol reagent according to the manufacturer's protocol. Total RNA (4 μg) was reverse transcribed using the SuperScript III First-Strand Synthesis System for RT-PCR (Invitrogen) and random hexamers, according to the manufacturer's protocol. Real time quantitative PCR of the cDNA template was performed in an iCycler (Bio-Rad). *VEGF* and *GAPDH* primers were from SABiosciences (Frederick, MD). The PCR contained 150 ng of cDNA, 10 μM forward and reverse primers, and 12.5 μl of 2× RT^2 Real Time SYBR Green PCR Master mix (SABiosciences) in a total volume of 25 μl. All PCR were performed in triplicate. Results were calculated as expression of the target gene relative to expression of the reference gene (*GAPDH*).

MAEC tube formation assay

24-well tissue culture plates were coated with 250μl of Growth Factor-Reduced Matrigel (BD Bioscience, San Diego, CA) and incubated at 37°C for 30min. When the Matrigel solidified, 1.25×10^5 of WT mouse aortic endothelial cells (MAECs) were added to each well in 250 μl of chosen PMN-conditioned DMEMF-12 medium obtained as described in "Regulation of VEGF in PMNs" and supplemented with 10% FBS, 90μg/ml heparin. Inhibitors of VEGF, neutralizing LEAF™ rat anti-mouse VEGF mAb (Biolegend), isotype matched rat IgG_{2a} (100 μg/ml) (Biolegend) and recombinant mouse sFLT-1 (R&D Systems) (100ng/ml), were preincubated for 60 min with conditioned media of WT TNFα-stimulated PMNs before its addition to MAECs. Live time-lapse photography was performed for 12h, using 5min intervals on Leica DMIRB Inverted Microscope equipped with Roper Scientific CoolSNAP HQ Cooled CCD camera, temperature Controller and CO_2 incubation Chamber. Snapshots were taken using MetaMorph Software. Tube formation was analyzed and quantified using ImageJ 1.34 software.

Statistical analysis

Data are expressed as means ± SEM. To determine significance, a one way ANOVA test was performed to compare angiogenic responses between the three mouse genotypes and a two-tailed Student's t-test was performed for comparisons between WT and the $\alpha_M^{-/-}$ mice using the Sigma-Plot software program (SPSS). P<0.05 was considered to be statistically significant.

Results

Integrin $\alpha_M\beta_2$ is critical in angiogenesis in vivo

Leukocytes, particularly PMNs and macrophages, are important supporters of angiogenesis as a source of proteases and angiogenic factors (reviewed in (1, 2)). The β_2 integrins are crucial in regulation of a variety of leukocyte responses including adhesion, migration and cytokine production (reviewed in (13)). Accordingly, we examined the role of two prominent members of the β_2 integrin subfamily, $\alpha_M\beta_2$ and $\alpha_L\beta_2$, in angiogenesis. These two integrins share the same β_2 subunit and their α-subunits are 49% identical (19). Angiogenesis was analyzed in the $a_M^{-/-}$, $\alpha_L^{-/-}$ and control WT mice using two tumor models, murine B16F10 melanoma and RM1 prostate cancer. These tumors are known to be highly vascularized, and their growth is heavily dependent upon an angiogenic response (20, 21). Staining of tumor sections for endothelial cells with CD31 (green fluorescence) revealed normal, well-developed, thick vasculature in tumors grown in the $\alpha_L^{-/-}$ and WT mice. In contrast, angiogenesis was significantly impaired in $\alpha_M^{-/-}$ mice as only a few short and thin vessel-like structures were observed in melanomas and prostate tumors from these mice (Fig. 1A). Blood vessel area of the melanoma sections was attenuated by ~70% in the $\alpha_M^{-/-}$ compared to tumors in the $\alpha_L^{-/-}$ and WT mice (P<0.001, n=8 per group) (Fig. 1B, upper panel). Also, significantly reduced vascular area was observed in RM1 prostate tumors grown in $\alpha_M^{-/-}$ mice compared to $\alpha_L^{-/-}$ and WT mice: 6200 μm^2 ± 1000 vs 12800 ± 2000 in $\alpha_L^{-/-}$ and 12000 ± 2150 μm^2 in WT mice (P<0.01, n=8 per group) (Fig. 1B, lower panel). Consistent with the blunted angiogenic response in the $\alpha_M^{-/-}$ mice, melanomas grown in these mice were 70–80% smaller (P<0.01, n=7 per group) than those derived in the $\alpha_L^{-/-}$ and WT mice: 40±10 mg in $\alpha_M^{-/-}$ vs 202±42 mg in WT and 178±34 mg in $\alpha_L^{-/-}$ mice. Additionally, the average weight of RM1 prostate tumors recovered from the $\alpha_M^{-/-}$ mice was ~40–50% lower than from the $\alpha_L^{-/-}$ and WT mice (P<0.05, n=8 per group): 295±30 mg in $\alpha_M^{-/-}$ vs 497±80 mg in WT and 570±100 mg in $\alpha_L^{-/-}$ mice (Fig. 1C&D).

Impaired angiogenesis in the $\alpha_M^{-/-}$ mice was corroborated using Matrigel as a third angiogenic model. Mice were injected with Matrigel alone or with Matrigel supplemented with VEGF or KC (keratinocyte-derived factor) to stimulate angiogenesis. CD31 staining of Matrigel plugs containing VEGF or KC, revealed well-formed vasculature in the implants from WT and $\alpha_L^{-/-}$ mice while the Matrigel plugs from $\alpha_M^{-/-}$ mice showed no distinct vascular formations although a few CD31-positive ECs were discerned within the plugs (Fig. 1E). Also, regardless of the angiogenic factor used, blood vessel area in the Matrigel implants in the $\alpha_M^{-/-}$ mice was reduced by ~75% compared to the implants from the $\alpha_L^{-/-}$ and WT animals (P<0.01, n=8 per group) (Fig. 1F). In control Matrigel plugs without

proangiogenic cytokines, no blood vessels were detected in any of the three mouse genotypes tested (data not shown).

The neovasculature in $\alpha_M^{-/-}$ mice is immature

The presence of smooth muscle cells and pericytes within vasculature is a key indicator of its maturity since they stabilize blood vessels. We double-stained melanoma and prostate tumor sections with Abs to CD31 and to smooth muscle cell actin (SMA, Fig. 2A top panel) or to NG2 chondroitin sulfate proteoglycan, a marker of pericytes (Fig, 2A bottom panel). In prostate tumors grown in WT and $\alpha_L^{-/-}$ mice 30–37% of total CD31$^+$ blood vessels stained for SMA, whereas only 15% of blood vessels formed in $\alpha_M^{-/-}$ mice expressed this marker ($P<0.02$, n=8) (Fig. 2B). Costaining for CD31 and NG2 revealed reduced pericytes interacting with blood vessels in prostate tumors in $\alpha_M^{-/-}$ mice as compared to WT and $\alpha_L^{-/-}$ mice (25% NG2-positive blood vessels in $\alpha_M^{-/-}$ vs 50–58% in $\alpha_L^{-/-}$ and WT mice, ($P<0.05$, n=8) (Fig. 2C). Measurement of blood vessel diameter revealed that they were substantially smaller in prostate tumors of $\alpha_M^{-/-}$ mice as compared to WT and $\alpha_L^{-/-}$ mice (25±8μm vs 50–55±10m, $P<0.05$, n=60, 4 mice per group) (Fig. 2D, top panel & E). Also, immunostaining for laminin showed 50% reduction basement membrane thickness of blood vessel in $\alpha_M^{-/-}$ mice (2.7±0.3μm) compared to WT and $\alpha_L^{-/-}$ mice (5.8–6 ±1.3 μm, $P<0.03$, n=60, 4 mice per group; Fig. 2D lower panel & F). With decreased maturation and laminin deposition, we considered that vasculature in $\alpha_M^{-/-}$ mice might be leaky. Plasma leakage measured as an area positive for plasma-derived fibrin was enhanced by 2.5-fold in tumors grown in $\alpha_M^{-/-}$ mice compared with WT and $\alpha_L^{-/-}$ mice (13.8 ±1.8% vs 5.2 ± 1.1% and 3.8± 0.7% respectively, $P<0.03$, n=20, 4 mice per group; Fig. 2G&H). The vasculature in melanoma tumors grown in $\alpha_M^{-/-}$ mice also showed reduced maturity and leakiness (data not shown). In addition, the permeability of preexisting blood vessels in dorsal skin of $\alpha_M^{-/-}$ and WT mice was examined using Evans Blue dye injected intravenously. Baseline permeability upon injection of control PBS as well as VEGF-A-induced vascular permeability were similar in $\alpha_M^{-/-}$ and WT mice indicating that preexisting vasculature in $\alpha_M^{-/-}$ mice was normal (Supplemental Fig. 1).

Impaired PMN and macrophage recruitment to angiogenic sites in $\alpha_M^{-/-}$ mice

The CD11b$^+$/Gr-1$^+$ myeloid cells consisting primarily of PMNs are crucial enhancers of angiogenesis and contribute to angiogenic switch in many tumors (4, 5, 22). Since tumor growth and angiogenesis were impaired in the $\alpha_M^{-/-}$ (CD11b$^{-/-}$) mice, we considered the possibility that this integrin may regulate recruitment of these cells to growing tumors. First, we examined infiltration of CD11b$^+$/Gr-1$^+$ cells in prostate and melanoma tumors in WT and $\alpha_L^{-/-}$ mice by double staining with anti-CD11b (green) and anti-Ly6G (Gr-1) mAbs (red). As shown in Fig. 3A, 70–80% of CD11b$^+$ cells were also positive for Gr-1, and numerous CD11b$^+$/Gr-1$^+$ cells were detected in prostate tumors in WT and $\alpha_L^{-/-}$ mice with no differences in their recruitment observed in the two mouse strains. Similar results were obtained with melanoma tumors (data not shown). Since assessment of CD11b$^+$/Gr-1$^+$ cell recruitment to tumors in $\alpha_M^{-/-}$ (CD11b$^{-/-}$) mice was not feasible due to the absence of the α_M integrin subunit on these cells, we stained tumor sections only with PMN-specific anti-Ly6G (Gr-1) mAb. Indeed, PMN infiltration into both melanoma and prostate tumors was significantly reduced in the $\alpha_M^{-/-}$ mice compared to WT and $\alpha_L^{-/-}$ littermates (Fig. 3B).

Quantification of Ly6G-positive areas in tumor sections verified these observations: 900μm^2 ± 210 in $\alpha_M^{-/-}$ vs 3600μm^2 ± 1120 in WT and 3950μm^2 ± 350 in $\alpha_L^{-/-}$ mice in melanomas (P<0.02, n=8) and 1200μm^2 ± 265 in $\alpha_M^{-/-}$ vs 6020μm^2 ± 840 in WT and 7135μm^2 ± 1780 in $\alpha_L^{-/-}$ mice in prostate tumors (P< 0.01, n=8 per group) (Fig. 3C). Next, tumor sections were stained with the monocyte/macrophage-specific mAb (MOMA-2). Macrophage infiltration into both tumors was decreased by 50–60 % in the $\alpha_M^{-/-}$ mice as compared to WT and $\alpha_L^{-/-}$ littermates (Fig. 3D&E). In melanomas grown in the $\alpha_M^{-/-}$ mice: macrophage-positive area was 1820μm^2 ± 160 compared to 5610μm^2 ± 985 in WT and 5240μm^2 ± 450 in $\alpha_L^{-/-}$ mice, whereas in prostate tumors it was 3600μm^2 ± 750 in $\alpha_M^{-/-}$ mice vs 7500μm^2 ± 1100 in WT and 7280μm^2 ± 1300 in $\alpha_L^{-/-}$ littermates (P<0.05, n=8 per group) (Fig. 3E). In addition, staining of Matrigel implant sections with anti-PMN and MOMA-2 Abs revealed robust VEGF- and KC-dependent leukocyte infiltration into the centers of the implants in WT and $\alpha_L^{-/-}$ mice while it was inhibited in the $\alpha_M^{-/-}$ mice (data not shown).

Bone marrow transplantation (BMT) and suppression with blocking antibodies confirm the importance of $\alpha_M\beta_2$ in angiogenesis

Next, we sought to confirm that reduced tumor growth and angiogenesis in the $\alpha_M^{-/-}$ mice are due to impaired functions of bone marrow-derived cells (BMDC) including leukocytes, and are not caused by defective vascular cells. Thus, we performed bone marrow transplant (BMT) experiments and examined growth and angiogenesis in RM1 tumors. Transplantation of $\alpha_M^{-/-}$ BM into WT hosts (α_M^{-} $^{-}$ $\rightarrow$ WT) resulted in reduced RM1 tumor growth and angiogenesis (tumor weight: P=0.0169, vascular area: P=0.028 for $\alpha_M^{-/-} \rightarrow$ WT vs WT $\rightarrow$ WT, n=5) (Fig. 4A&B). Alternatively, transplantation of WT BM into the $\alpha_M^{-/-}$ hosts (WT $\rightarrow$ $_M^{-/-}$) restored growth and angiogenesis of prostate tumors to these of control WT mice receiving WT bone marrow (RM1 weight: P=0.0183, vascular area: P=0.012 for WT $\rightarrow$ $\alpha_M^{-/-}$ vs $\alpha^{M-/-}$; $\rightarrow$ WT, n=5) (Fig. 4A&B). These results suggest that blunted tumor growth and angiogenesis in the $\alpha_M^{-/-}$ mice is a consequence of altered BMDC functions. In addition, image analysis of RM1 tumor sections stained with PMN-specific anti-Ly6G and anti-monocyte/macrophage MOMA-2 antibodies revealed impaired recruitment of these cells to tumors grown in WT recipients receiving $\alpha_M^{-/-}$ BM as compared to control WT $\rightarrow$ WT mice, indicating a crucial role of $\alpha_M\beta_2$ in this process (P=0.0184 for PMNs (Ly6G) and P=0.0167 for MOMA-2, n=5) (Fig. 4C&D). In contrast, transplantation of WT BM to $\alpha_M^{-/-}$ recipients restored not only angiogenesis, but also PMN and macrophage migration into tumors (PMNs: P=0.021, MOMA-2: P=0.0454 for WT $\rightarrow \alpha_M^{-/-}$ vs $\alpha_M^{-/-} \rightarrow$ WT, n=5) (Fig. 4C&D). To exclude the possibility that α_M deficiency might impair recovery of the immune system upon BMT, we assessed engraftment efficiency 6 weeks after BMT in chimeric $\alpha_M^{-/-} \rightarrow$ WT and WT $\rightarrow \alpha_M^{-/-}$ mice using WT and $\alpha_M^{-/-}$ mice not undergoing BMT as controls. We have collected spleens and thymuses from these mice, prepared single cell suspensions and measured percentages of PMN, macrophage, B and T cells by flow cytometry using FITC-labeled Abs to cell specific markers (Ly-6G, F4/80, CD19, CD3, respectively) and FITC-labeled isotype-matched Abs as controls. We found that the content of individual leukocyte subsets was similar in respective organs in both chimeric mouse lines as well as in control mice (no BMT), indicating that α_M deficiency did not impact BMT engraftment efficiency (supplemental Table 1). In addition, flow cytometry of

circulating total leukocytes with anti-mouse α_M mAb confirmed its absence in the $\alpha_M^{-/-} \rightarrow$ WT chimeras and its presence in the WT $\rightarrow {}_M^{-/-}$ mice (data not shown). Also, to confirm the importance of the α_M integrin in angiogenesis, WT mice were injected with a rat anti-α_M blocking antibody (clone M1/70), that had been shown to specifically inhibit neointima formation in rabbits (23). These neutralizing antibodies bind to the ligand binding site within the α_M subunit and inhibit its interactions with ligands thereby mimicking the gene ablation. Matrigel implants were harvested after 8 days and the antibody was injected before Matrigel injection and then every 2 days. Vasculature was analyzed in Matrigel sections stained with anti-CD31 mAb (Fig. 4E). The anti-α_M antibody reduced KC-induced angiogenesis in Matrigel implants by~60–80% as compared to not injected mice, whereas isotype-matched normal rat IgG_{2b} had no effect indicating specificity ($P<0.05$ mice injected with anti-α_M vs not injected, n=4 mice per group) (Fig. 4E&F). Taken together, these experiments verify the importance of $\alpha_M\beta_2$ on myeloid cells in tumor-induced angiogenesis via regulation of leukocyte recruitment to sites of neovascularization.

$\alpha_M\beta_2$ facilitates leukocyte recruitment to angiogenic sites via interaction with Plg and enhancement of Plg activation

As Plm-dependent ECM proteolysis greatly facilitates leukocyte invasion (10–12), we hypothesized that the inability of $\alpha_M^{-/-}$ leukocytes to invade tumors could be caused by impaired Plg activation on the leukocyte surface. Since $\alpha_M\beta_2$ and $\alpha_L\beta_2$ are the most abundant β_2-integrins on PMNs and macrophages, we used a modified Boyden chamber system to elucidate the role of $\alpha_M\beta_2$ and $\alpha_L\beta_2$ in mouse peritoneal PMN and macrophage migration through a Matrigel matrix barrier (ECM extracted from Engelbreth-Holm-Swarm (EHS) mouse sarcoma) in response to KC (Fig. 5A&B). In the absence of KC, there was minimal migration of leukocytes into the lower chambers in the presence or absence of added Plg. However, although KC-induced migration of PMNs and macrophages was significantly impeded by Matrigel, this barrier effect was overcome by addition of Plg to the $\alpha_L^{-/-}$ and WT leukocytes (Figs. 5A&B). In contrast, addition of Plg to the $\alpha_M^{-/-}$ cells failed to improve their migration through the Matrigel barrier, suggesting that the capability of these cells to bind and activate Plg was limited ($P=0.014$ $\alpha_M^{-/-}$ vs WT PMNs and $P=0.005$ $\alpha_M^{-/-}$ vs WT macrophages, n=3) (Fig. 5A&B). Indeed, flow cytometry showed a 50–60% reduction in binding of Alexa488-conjugated soluble Plg to $\alpha_M^{-/-}$ peritoneal PMNs and macrophages as compared to WT and $\alpha_L^{-/-}$ leukocytes (Fig. 5C).

To determine whether Plg interacts directly with the α_MI- and α_LI- domain, the major site of ligand binding in β_2 integrins (13), we performed SPR experiments. GST-tagged α_MI-domain interacted with Plg immobilized on biosensor chips in a concentration-dependent manner while the GST-tagged α_LI-domain did not bind Plg (Fig. 5D). GST alone also did not interact with Plg. From the progress curves of the Plg:α_MI-domain interaction, we estimated a $Kd = 1.76 \pm 0.9 \times 10^{-7}$. This value was derived by fitting the kinetic data to a 1:1 global Langmuir model, and the stoichiometry observed at ligand saturation was 1:1.

Next, we compared Plg activation on the surface of WT, $\alpha_L^{-/-}$ and $\alpha_M^{-/-}$ leukocytes using a fluorogenic plasmin-specific peptide substrate. Peripheral blood PMNs and lymphocytes were stimulated with KC and pretreated with sc-uPA to activate the integrin and enable sc-

uPA binding to leukocyte surface, respectively. No plasmin activity was detected in the absence of leukocytes. The $\alpha_M^{-/-}$ PMNs showed a 50% reduction in Plm generation as compared to WT and $\alpha_L^{-/-}$ PMNs ($P<0.03$, n=5) (Fig. 5E). In contrast, Plg activation was similar on WT, $\alpha_M^{-/-}$ and $\alpha_L^{-/-}$ lymphocytes (Fig. 5E). As with PMNs, peritoneal α_M-deficient macrophages also exhibited severely reduced (by 75%) Plg activation compared to the $\alpha_L^{-/-}$ and WT macrophages ($P<0.05$, n=5) (Fig. 5F). In control experiments, we examined α_L expression on α_M-deficient PMN, α_M levels on α_L-null and control WT PMNs (both peritoneal and circulating) by flow cytometry. Neither α_L- nor α_M-deficiency altered expression of its counterpart β_2-integrin on PMNs (data not shown), confirming that Plg recognition and activation is $\alpha_M\beta_2$-specific. Taken together, $\alpha_M\beta_2$ functions as a Plg receptor and this function is critical in Plm-dependent leukocyte recruitment to angiogenic sites.

$\alpha_M\beta_2$ regulates secretion of VEGF-A by PMNs

Our data demonstrate a critical role of $\alpha_M\beta_2$ in leukocyte recruitment to angiogenic sites. However, we considered a possibility that $\alpha_M\beta_2$ might also regulate other proangiogenic leukocyte functions such as production/secretion of angiogenic stimulators. The $CD11b^+$/$Gr\text{-}1^+$ cells, that primarily constitute PMNs, are of particular interest as they secrete high levels of MMP-9 and VEGF leading to “angiogenic switch” in many tumors and to a failure of anti-VEGF therapies (5, 22). Thus, we compared the VEGF-A content of supernatants released from peripheral blood PMN of WT and $\alpha_M^{-/-}$ and $\alpha_L^{-/-}$ mice. In the absence of TNFα stimulation, VEGF-A levels were low and similar in PMNs of all three genotypes. Notably, upon stimulation with TNFα, VEGF-A content was substantially lower (by~60%) in the $\alpha_M^{-/-}$ PMN-conditioned medium compared to medium harvested from WT or $\alpha_L^{-/-}$ PMNs ($P<0.05$, n=6) (Fig. 6A). VEGF is stored in specific granules in human PMNs (24). To determine whether $\alpha_M\beta_2$ regulates *de novo* synthesis of VEGF or/and its secretion, we utilized cycloheximide, an inhibitor of protein synthesis, and pentoxifylline, an inhibitor of PMN degranulation. Cycloheximide did not affect VEGF content in supernatants of TNFα-stimulated PMNs of any mouse strains tested, suggesting that TNFα did not stimulate *de novo* VEGF synthesis (Fig. 6A). This interpretation was corroborated by qRT-PCR assays, which revealed that VEGF mRNA levels were similar not only in resting and TNFα-treated PMNs but also in WT, $\alpha_M^{-/-}$ and $\alpha_L^{-/-}$ PMNs (Table 1). In contrast, pentoxifylline inhibited secretion of VEGF from PMNs and reduced its concentration by 80–85% in supernatants from WT and $\alpha_L^{-/-}$ PMNs and by additional 20% from $\alpha_M^{-/-}$ PMNs (Fig. 6A). Taken together, these data suggest that $\alpha_M\beta_2$ integrin does not regulate VEGF synthesis but rather its secretion via control of PMN degranulation, consistent with prior data implicating $\alpha_M\beta_2$ in degranulation of human PMNs ex vivo (25). To corroborate this conclusion, we measured the concentration of lactoferrin, a marker of PMN specific granules, in PMN supernatants. The relative changes of lactoferrin and VEGF in the PMN-conditioned media were very similar. Importantly, the $\alpha_M^{-/-}$ PMNs, but not the $\alpha_L^{-/-}$ PMNs, showed severely impaired release of lactoferrin into the supernatants of TNFα-stimulated $\alpha_M^{-/-}$ PMNs, which were almost as low as in supernatants of resting PMNs from each mouse strain (Supplemental Fig. 2). We also sought to examine VEGF production/secretion in $CD117^+$ progenitor cells isolated from bone marrow of WT, $\alpha_M^{-/-}$ and $\alpha_L^{-/-}$ mice. However, we failed to detect mRNA for VEGF in these immature cells.

Next, we analyzed the capacity of WT mouse aortic endothelial cells (MAEC) to form tubes in the presence of the conditioned media derived from WT, $\alpha_M^{-/-}$ or $\alpha_L^{-/-}$ TNFα-stimulated PMNs. MAEC in the presence of media collected from WT or $\alpha_L^{-/-}$ PMNs formed well-organized tube-like networks. In contrast, tubes formed by MAECs in the presence of the $\alpha_M^{-/-}$ PMN-conditioned media were incomplete ($P<0.05$, n=20) (Fig. 6 B&C). In control samples, TNFα alone did not support tube formation by ECs. In order to confirm that tube formation by MAEC in the presence of WT or $\alpha_L^{-/-}$ PMN supernatants is VEGF-dependent, we added neutralizing rat anti-mouse VEGF mAb (clone 2G11-2A05), or its isotype control rat IgG_{2a}, or soluble VEGF receptor-1 (sFLT-1). The effectiveness of both of these VEGF inhibitors has been previously established (e.g. (26, 27)). These inhibitors of VEGF almost completely inhibited (by 75–80%) tube formation by MAEC ($P<0.05$, n=20). In contrast, the isotype control antibody did not have any effect (Fig. 6B bottom panel, & C). Although other pro-angiogenic factors are likely to be present in PMN supernatants, VEGF does appear to be the key stimulator of this process in our experimental system. Finally, supplementation of $\alpha_M^{-/-}$ PMN conditioned medium with recombinant mouse VEGF to the same concentration as in medium from WT PMNs (520 pg/ml) enhanced the numbers of closed tubes by 2.5-fold and almost completely restored MAEC tube formation (Fig. 6B, top panel). Taken together, $\alpha_M\beta_2$ does not directly regulate VEGF-A *de novo* synthesis. However, it enhances VEGF-A secretion from PMN intracellular stores via its enhancement of PMN degranulation.

Discussion

The goal of this study was to examine involvement of the two major leukocyte β_2 integrins, $\alpha_M\beta_2$ and $\alpha_L\beta_2$, in angiogenesis. Using the α_M- and α_L-deficient mice, we demonstrate that $\alpha_M\beta_2$ promotes angiogenesis in model melanoma and prostate tumors, as well as in Matrigel implants, while the $\alpha_L\beta_2$ integrin does not. Blood vessel formation and tumor growth were impaired in $\alpha_M^{-/-}$ mice as compared to the $\alpha_L^{-/-}$ or WT mice. Impaired angiogenesis in $\alpha_M^{-/-}$ mice was due to dramatic reduction in recruitment of PMNs and macrophages into the tumors and Matrigel implants. Furthermore, we showed that Plg binding and activation on the surface of $\alpha_M^{-/-}$ PMNs and macrophages as well as their Plm-dependent invasion through Matrigel were significantly attenuated as compared to the $\alpha_L^{-/-}$ and WT cells. These data were consistent with the SPR sensograms showing that recombinant α_MI-domain directly interacts with Plg, but the α_LI-domain does not. These findings are in concord with prior studies showing that $\alpha_M\beta_2$ recognizes urokinase (uPA) and Plg enhancing their reciprocal activation on PMN surface (14, 15, 28). To our knowledge this is the first report implicating $\alpha_M\beta_2$ in angiogenesis and demonstrating its intimate interplay with Plg *in vivo*. Although, the β_2-deficient mice showed slowed angiogenesis in healing wounds (29), none of the individual β_2 integrin family members was shown to contribute to this process. The implication of $\alpha_M\beta_2$ in angiogenesis and Plg binding/activation is quite specific as $\alpha_L\beta_2$ did not show any impairment in these responses. This distinction may be explained, at least in part, by the relatively low sequence identity between the ligand binding α_MI- and α_LI-domains resulting in the $\alpha_M\beta_2$ promiscuity for many structurally unrelated ligands, while $\alpha_L\beta_2$ shows a very limited ligand repertoire with little overlap in ligand recognition with $\alpha_M\beta_2$ (19). With regard to ligand repertoire, the two β_2 integrins, $\alpha_X\beta_2$ and $\alpha_D\beta_2$, are more

similar to $\alpha_M\beta_2$ than $\alpha_L\beta_2$, and it would be interesting to examine their role in angiogenesis. The critical role of $\alpha_M\beta_2$-dependent Plg activation in PMN and macrophage recruitment to angiogenic niches is in accord with previous studies demonstrating the importance of cell-bound plasmin in leukocyte recruitment in a variety of *in vivo* models of inflammation (10–12), and also with crucial role of the Plg system in angiogenesis (30–36). Pericellular proteolysis is critical for initiation of angiogenesis as evidenced by suppression of neovascularization in mice deficient in various proteases (31, 37–39) and by administration of a variety of protease inhibitors (40, 41). Among the proteases implicated in angiogenesis, in addition to plasmin, are its activators and metalloproteinases (reviewed in (4, 8)). Plasmin is one of pro-MMP-9 activators (42) and PMN-derived MMP-9 is responsible for angiogenic switch in some tumors (5). Consistent with decreased Plm activity and the capacity of $\alpha_M\beta_2$ to bind and activate MMP-9 (43), we observed reduced MMP-9 activity in tumor extracts from the $\alpha_M^{-/-}$ mice (data not shown).

As a key source of proteases and proangiogenic factors, PMNs and macrophages are essential for angiogenesis. Angiogenesis is severely blunted in neutropenic mice (5, 29, 44, 45) or in mice in which macrophages have been eliminated (2). Robust PMN and macrophage recruitment is observed into ischemic tissues including tumors (46), and in many tumors recruitment of these cells tumors correlates with poor host survival (reviewed in (2)). With such evidence, the virtual absence of PMNs and macrophages in the angiogenic tissue of the $\alpha_M^{-/-}$ mice provides a mechanism to account for profound reduction in neovascularization and tumor growth in these animals. In addition to defective recruitment, the $\alpha_M^{-/-}$ PMNs also exhibited severely attenuated secretion of VEGF-A due to impaired degranulation, and supernatants collected from these cells did not support EC tube formation in *in vitro* assays. As enhanced VEGF is the hallmark and a key contributor to $CD11b^+$/$Gr\text{-}1^+$ (mostly PMNs)-dependent resistance of many tumors to VEGF targeting anti-cancer therapies, we have focused our investigations on the regulation of this pivotal cytokine. However, we can not exclude, that other pro-angiogenic factors, particularly those stored in PMN granules, might also be regulated by $\alpha_M\beta_2$ via its influence on degranulation. This important issue is open for further investigation. Even if $\alpha_M^{-/-}$ PMNs had been able to migrate, they would likely to have failed to promote angiogenesis due to an inability to supply of the requisite amounts of the major pro-angiogenic stimulus, VEGF. The neovasculature in growing tumors, but not preexisting blood vessels, in $\alpha_M^{-/-}$ mice showed immature and leaky phenotype. This might be caused by insufficient infiltration of $CD11b^+$/$Ly6G^+$ PMNs known to support vascular maturation via elevated levels of proangiogenic factors VEGF and MMP-9 (22).

Taken together, our studies demonstrate that integrin $\alpha_M\beta_2$ promotes angiogenesis *in vivo* via dual mechanism: first, as a Plg receptor, $\alpha_M\beta_2$ supports Plm-dependent recruitment of myeloid cells to angiogenic niches; second, $\alpha_M\beta_2$ enhances VEGF-A secretion by PMN degranulation. Based on our findings, selective antagonists of $\alpha_M\beta_2$ may be considered as a new target to inhibit tumor angiogenesis.

Supplementary Material

Refer to Web version on PubMed Central for supplementary material.

Acknowledgments

We thank Dr. Tatiana Byzova for expertise and advice regarding the *in vivo* angiogenesis models.

This work was supported by funding from NIAID (AIO 80596 to D.A.S.) AHA SDG 0335088N to E.P., NIH grants from the Heart, Lung and Blood Institute (R01 HL17964 and P01 HL07331 to E.F.P.).

Nonstandard abbreviations used

MAEC	mouse aortic endothelial cells
KC	keratinocyte-derived cytokine
VEGF-A	vascular endothelial growth factor A
Plg	plasminogen
Plm	plasmin
PMNs	neutrophils
sc-uPA	single-chain urokinase-type plasminogen activator
SMA	smooth muscle cell actin
NG2	neural/glial antigen 2
BMT	bone marrow transplantation

References

1. Tazzyman S, Niaz H, Murdoch C. Neutrophil-mediated tumour angiogenesis: subversion of immune responses to promote tumour growth. Semin Cancer Biol. 2013; 23:149–158. [PubMed: 23410638]
2. Qian B-Z, Pollard JW. Macrophage diversity enhances tumor progression and metastasis. Cell. 2010; 141:39–51. [PubMed: 20371344]
3. Kusumanto YH, Dam WA, Hospers GA, Meijer C, Mulder NH. Platelets and granulocytes, in particular the neutrophils, form important compartments for circulating vascular endothelial growth factor. Angiogenesis. 2003; 6:283–287. [PubMed: 15166496]
4. Noonan DM, De Lerma Barbaro A, Vannini N, Mortara L, Albini A. Inflammation, inflammatory cells and angiogenesis: decisions and indecisions. Cancer Metastasis Rev. 2008; 27:31–40. [PubMed: 18087678]
5. Nozawa H, Chiu C, Hanahan D. Infiltrating neutrophils mediate the initial angiogenic switch in a mouse model of multistage carcinogenesis. Proc Natl Acad Sci U S A. 2006; 103:12493–12498. [PubMed: 16891410]
6. Van Hinsbergh VWM, Engelse MA, Quax PHA. Pericellular Proteases in Angiogenesis and Vasculogenesis. Arterioscler Thromb Vasc Biol. 2006; 26:716–728. [PubMed: 16469948]
7. Lee S, Zheng M, Kim B, Rouse BT. Role of matrix metalloproteinase-9 in angiogenesis caused by ocular infection with herpes simplex virus. J Clin Invest. 2002; 110:1105–1111. [PubMed: 12393846]
8. Shamamian P, Schwartz JD, Pocock BJ, Monea S, Whiting D, Marcus SG, Mignatti P. Activation of progelatinase A (MMP-2) by neutrophil elastase, cathepsin G, and proteinase-3: arole for inflammatory cells in tumor invasion and angiogenesis. J Cell Physiol. 2001; 189:197–206. [PubMed: 11598905]
9. Das R, Pluskota E, Plow EF. Plasminogen and its receptors as regulators of cardiovascular inflammatory responses. Trends Cardiovasc Med. 2010; 20:120–124. [PubMed: 21335281]

10. Ploplis VA, French EL, Carmeliet P, Collen D, Plow EF. Plasminogen deficiency differentially affects recruitment of inflammatory cell populations in mice. Blood. 1998; 91:2005–2009. [PubMed: 9490683]
11. Busuttil SJ, Ploplis VA, Castellino FJ, Tang L, Eaton JW, Plow EF. A central role for plasminogen in the inflammatory response to biomaterials. J Thromb Haemost. 2004; 2:1798–1805. [PubMed: 15456492]
12. Swaisgood CM, Aronica MA, Swaidani S, Plow EF. Plasminogen is an important regulator in the pathogenesis of a murine model of asthma. Am J Respir Crit Care Med. 2007; 176:333–342. [PubMed: 17541016]
13. Tan SM. The leucocyte beta2 (CD18) integrins: the structure, functional regulation and signalling properties. Biosci Rep. 2012; 32:241–269. [PubMed: 22458844]
14. Pluskota E, Solovjov DA, Plow EF. Convergence of the adhesive and fibrinolytic systems: recognition of urokinase by integrin αMβ2 as well as by the urokinase receptor regulates cell adhesion and migration. Blood. 2003; 101:1582–1590. [PubMed: 12393547]
15. Pluskota E, Soloviev DA, Bdeir K, Cines DB, Plow EF. Integrin αMβ2 orchestrates and accelerates plasminogen activation and fibrinolysis by neutrophils. J Biol Chem. 2004; 279:18063–18072. [PubMed: 14769799]
16. Lu H, Smith CW, Perrard J, Bullard D, Tang L, Entman ML, Beaudet AL, Ballantyne CM. LFA-1 is sufficient in mediating neutrophil emigration in Mac-1 deficient mice. J Clin Invest. 1997; 99:1340–1350. [PubMed: 9077544]
17. Passaniti A, Taylor RM, Pili R, Guo Y, Long PV, Haney JA, Pauly RR, Grant DS, Martin GR. A simple, quantitative method for assessing angiogenesis and antiangiogenic agents using reconstituted basement membrane, heparin, and fibroblast growth factor. Lab Invest. 1992; 67:519–528. [PubMed: 1279270]
18. Cotter MJ, Norman KE, Hellewell PG, Ridger VC. A novel method for isolation of neutrophils from murine blood using negative immunomagnetic separation. Am J Pathol. 2001; 159:473–481. [PubMed: 11485906]
19. Ustinov VA, Plow EF. Identity of the amino acid residues involved in C3bi binding to the I-domain supports a mosaic model to explain the broad ligand repertoire of integrin alpha M beta 2. Biochemistry. 2005; 44:4357–4364. [PubMed: 15766265]
20. Huang X, Raskovalova T, Lokshin A, Krasinskas A, Devlin J, Watkins S, Wolf SF, Gorelik E. Combined antiangiogenic and immune therapy of prostate cancer. Angiogenesis. 2005; 8:13–23. [PubMed: 16132614]
21. van der Schaft DW, Dings RP, de Lussanet QG, van Eijk LI, Nap AW, Beets-Tan RG, Bouma-Ter Steege JC, Wagstaff J, Mayo KH, Griffioen AW. The designer anti-angiogenic peptide anginex targets tumor endothelial cells and inhibits tumor growth in animal models. FASEB J. 2002; 16:1991–1993. [PubMed: 12397082]
22. Jablonska J, Leschner S, Westphal K, Lienenklaus S, Weiss S. Neutrophils responsive to endogenous IFN-beta regulate tumor angiogenesis and growth in a mouse tumor model. J Clin Invest. 2010; 120:1151–1164. [PubMed: 20237412]
23. Rogers C, Edelman ER, Simon DI. A mAb to the β_2-leukocyte integrin Mac-1 (CD11b/CD18) reduces intimal thickening after angioplasty or stent implantation in rabbits. Proc Natl Acad Sci USA. 1998; 95:10134–10139. [PubMed: 9707613]
24. Gaudry M, Bregerie O, Andrieu V, El BJ, Pocidalo MA, Hakim J. Intracellular pool of vascular endothelial growth factor in human neutrophils. Blood. 1997; 90:4153–4161. [PubMed: 9354686]
25. Richter J, Ng-Sikorski J, Olsson I, Andersson T. Tumor necrosis factor-induced degranulation in adherent human neutrophils is dependent on CD11b/CD18-integrin-triggered oscillations of cytosolic free Ca2+ Proc Natl Acad Sci U S A. 1990; 87:9472–9476. [PubMed: 1979172]
26. Basu A, Contreras AG, Datta D, Flynn E, Zeng L, Cohen HT, Briscoe DM, Pal S. Overexpression of vascular endothelial growth factor and the development of post-transplantation cancer. Cancer Res. 2008; 68:5689–5698. [PubMed: 18632621]
27. Sossey-Alaoui K, Pluskota E, Davuluri G, Bialkowska K, Das M, Szpak D, Lindner DJ, Downs-Kelly E, Thompson CL, Plow EF. Kindlin-3 enhances breast cancer progression and metastasis by activating Twist-mediated angiogenesis. FASEB J. 2014; 28:2260–2271. [PubMed: 24469992]

28. Lishko VK, Novokhatny VV, Yakubenko VP, Skomorovska-Prokvolit HV, Ugarova TP. Characterization of plasminogen as an adhesive ligand for integrins αMβ2 (Mac-1) and 51 (VLA-5). Blood. 2004; 104:719–726. [PubMed: 15090462]
29. Schruefer R, Sulyok S, Schymeinsky J, Peters T, Scharffetter-Kochanek K, Walzog B. The proangiogenic capacity of polymorphonuclear neutrophils delineated by microarray technique and by measurement of neovascularization in wounded skin of CD18-deficient mice. J Vasc Res. 2006; 43:1–11. [PubMed: 16227701]
30. Oh C-W, Hoover-Plow J, Plow EF. The role of plasminogen in angiogenesis *in vivo*. J Thromb Haemost. 2003; 1:1683–1687. [PubMed: 12911578]
31. Heymans S, Luttun A, Nuyens D, Theilmeier G, Creemers E, Moons L, Dyspersin GD, Cleutjens JPM, Shipley M, Angellilo A, Levi M, Nübe O, Baker A, Keshet E, Lupu F, Herbert JM, Smits JFM, Shapiro SD, Baes M, Borgers M, Collen D, Daemen MJAP, Carmeliet P. Inhibition of plasminogen activators or matrix metalloproteinases prevents cardiac rupture but impairs therapeutic angiogenesis and causes cardiac failure. Nature Med. 1999; 5:1135–1142. [PubMed: 10502816]
32. Vogten JM, Reijerkerk A, Meijers JC, Voest EE, Borel RI, Gebbink MF. The role of the fibrinolytic system in corneal angiogenesis. Angiogenesis. 2003; 6:311–316. [PubMed: 15166500]
33. Drixler TA, Vogten JM, Gebbink MF, Carmeliet P, Voest EE, Borel RIH. Plasminogen mediates liver regeneration and angiogenesis after experimental partial hepatectomy. Br J Surg. 2003; 90:1384–1390. [PubMed: 14598419]
34. Creemers E, Cleutjens J, Smits J, Heymans S, Moons L, Collen D, Daemen M, Carmeliet P. Disruption of the plasminogen gene in mice abolishes wound healing after myocardial infarction. Am J Pathol. 2000; 156:1865–1873. [PubMed: 10854210]
35. Ling Q, Jacovina AT, Deora A, Febbraio M, Simantov R, Silverstein RL, Hempstead B, Mark WH, Hajjar KA. Annexin II regulates fibrin homeostasis and neoangiogenesis in vivo. J Clin Invest. 2004; 113:38–48. [PubMed: 14702107]
36. Chen PK, Chang BI, Kuo CH, Chen PS, Cho CF, Chang CF, Shi GY, Wu HL. Thrombomodulin functions as a plasminogen receptor to modulate angiogenesis. FASEB J. 2013; 27:4520–4531. [PubMed: 23943648]
37. Johnson C, Sung HI, Lessner SM, Fini ME, Galis ZS. Matrix metalloproteinase-9 is required for adequate angiogenic revascularization of ischemic tissues: potential role in capillary branching. Circ Res. 2004; 94:262–268. [PubMed: 14670843]
38. Masson V, de la Ballina LR, Munaut C, Wielockx B, Jost M, Maillard C, Blacher S, Bajou K, Itoh T, Itohara S, Werb Z, Libert C, Foidart JM, Noel A. Contribution of host MMP-2 and MMP-9 to promote tumor vascularization and invasion of malignant keratinocytes. FASEB J. 2005; 19:234–236. [PubMed: 15550552]
39. Ahn GO, Brown JM. Matrix metalloproteinase-9 is required for tumor vasculogenesis but not for angiogenesis:role of bone-marrow-derived myelomonocytic cells. Cancer Cell. 2008; 13:181–183. [PubMed: 18328420]
40. Pepper MS. Role of the Matrix Metalloproteinase and Plasminogen Activator-Plasmin Systems in Angiogenesis. Arterioscler Thromb Vasc Biol. 2001; 21:1104–1117. [PubMed: 11451738]
41. Stefanidakis M, Koivunen E. Cell-surface association between matrix metalloproteinases and integrins: role of the complexes in leukocyte migration and cancer progression. Blood. 2006; 108:1441–1450. [PubMed: 16609063]
42. Gong Y, Hart E, Shchurin A, Hoover-Plow J. Inflammatory macrophage migration requires MMP-9 activation by plasminogen in mice. J Clin Invest. 2008
43. Stefanidakis M, Ruohtula T, Borregaard N, Gahmberg CG, Koivunen E. Intacellular and cell surface localization of a complex between alphaMbeta2 integrin and promatrix metalloproteinase-9 progelatinase in neutrophils. J Immunol. 2004; 172:7060–7068. [PubMed: 15153528]
44. Benelli R, Morini M, Carrozzino F, Ferrari N, Minghelli S, Santi L, Cassatella M, Noonan DM, Albini A. Neutrophils as a key cellular target for angiostatin: implications for regulation of angiogenesis and inflammation. FASEB J. 2002; 16:267–269. [PubMed: 11772950]

45. Shaw JP, Chuang N, Yee H, Shamamian P. Polymorphonuclear neutrophils promote rFGF-2-induced angiogenesis in vivo. J Surg Res. 2003; 109:37–42. [PubMed: 12591233]

46. Cursiefen C, Chen L, Borges LP, Jackson D, Cao J, Radziejewski C, D'Amore PA, Dana MR, Wiegand SJ, Streilein JW. VEGF-A stimulates lymphangiogenesis and hemangiogenesis in inflammatory neovascularization via macrophage recruitment. J Clin Invest. 2004; 113:1040–1050. [PubMed: 15057311]

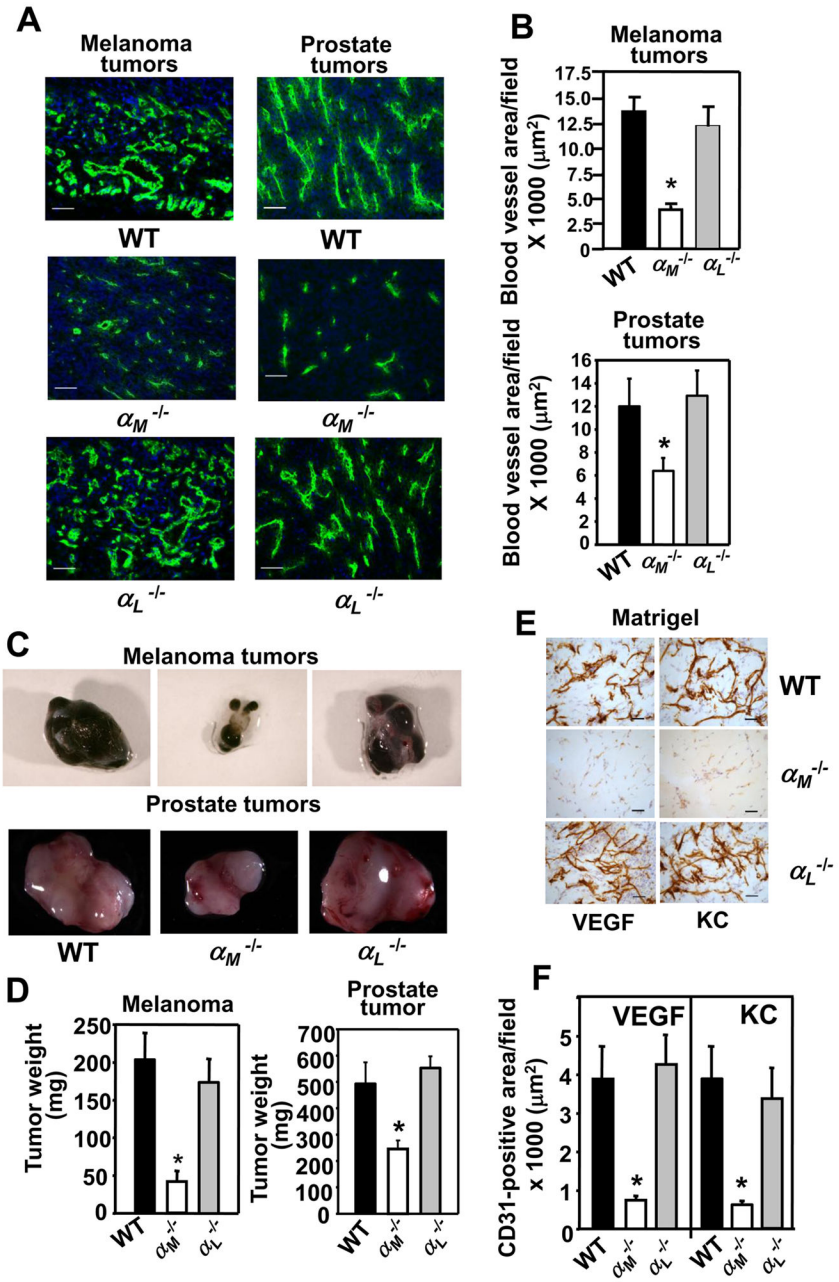

FIGURE 1.

Angiogenesis is impaired in the $\alpha_M^{-/-}$ mice. (A) Representative images of melanoma (left panel) and prostate (right panel) tumor sections stained with an EC marker, CD31 antibody (green), Scale bars, 50 μm. (B) Decreased area of CD31-stained vasculature in tumors grown in $\alpha_M^{-/-}$ mice. Data are representative of two independent experiments with 8 mice per group. (C&D). Average weight of melanoma and prostate tumors grown in $\alpha_M^{-/-}$ is lower than in WT mice and representative tumors are shown in C. Data are means ± SEM, (n= 8 mice per group) (E) Representative images of Matrigel implant sections stained with CD31 antibody. Scale bars, 50 μm. (F) Reduced area of CD31-positive vasculature in the

VEGF- or KC containing Matrigel implants from the $\alpha_M^{-/-}$ mice. The data are representative of 3 independent experiments with 8 mice per group.

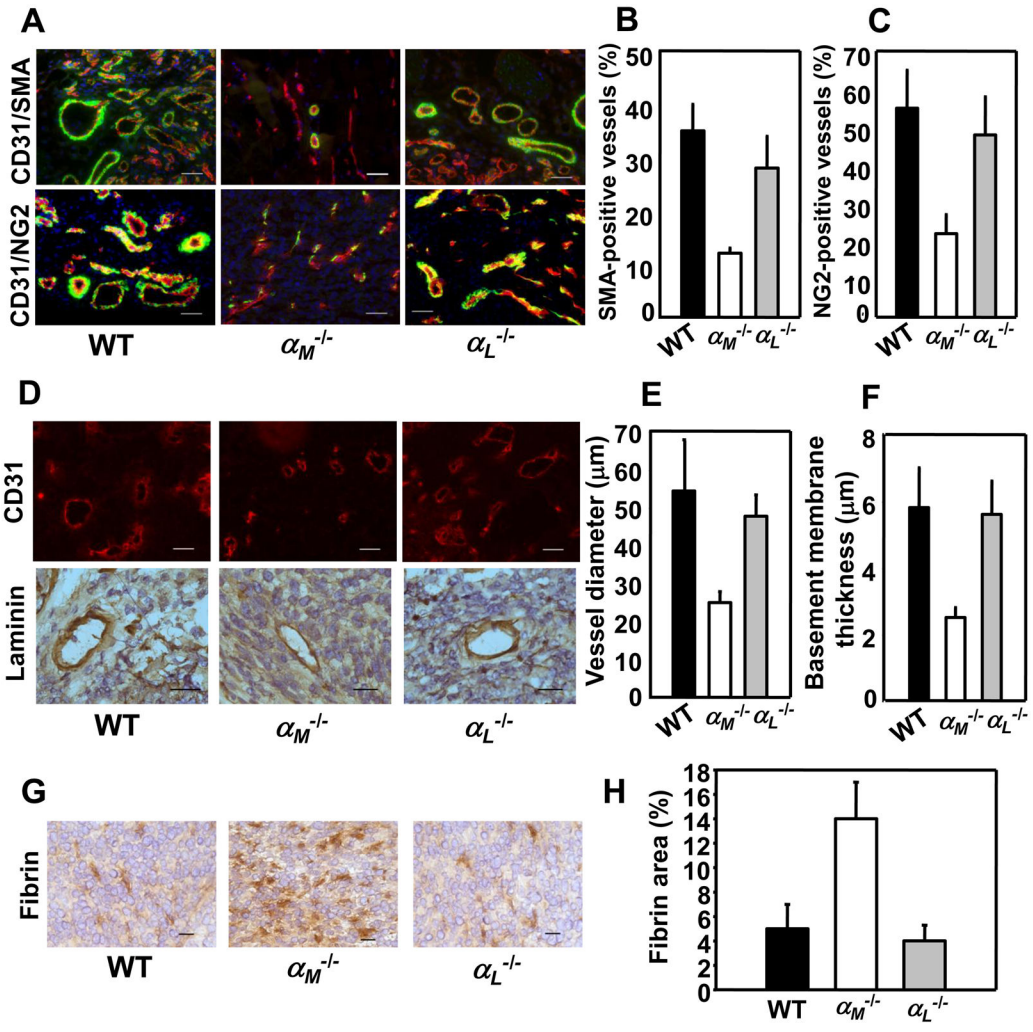

FIGURE 2.

Neovasculature in prostate tumors in $\alpha_M^{-/-}$ mice is immature and leaky. Immunohistochemistry and image analyses of RM1 prostate tumors implanted into WT, $\alpha_M^{-/-}$ and $\alpha_L^{-/-}$ mice. (A) Costaining for SMA (green) and CD31 (red; top panel) and for NG2 (green) and CD31 (red; bottom panel) in RM1 prostate tumors. Nuclei are stained with DAPI. Scale bars, 50 μm. (B&C) Quantification of the data presented in A top and bottom panel, respectively. Data are expressed as mean ± SEM and are representative of 3 independent experiments (n=8 mice/group). (D) CD31-stained (top panel) and laminin-stained (bottom panel) blood vessels in tumors grown in WT, $\alpha_M^{-/-}$ and $\alpha_L^{-/-}$ mice. Scale bars, 50 μm (top) and 25 μm (lower panel). (E) Vessel diameter was measured in 60 tumor vessels cut perpendicular to their longitudinal axis in 8 μm-thick sections, stained for CD31 from each mouse (4 mice/group). Data are expressed as mean ± SEM, n=60. (F) Thickness of laminin-positive basement membrane in blood vessels formed in WT, $\alpha_M^{-/-}$ and $\alpha_L^{-/-}$ mice. Data are mean ± SEM, n=60 and are representative of 3 independent experiments including 4 mice per group. (G) Representative photograph of fibrin content (brown) in tumors grown in WT, $\alpha_M^{-/-}$ and $\alpha_L^{-/-}$ mice. Scale bars, 25 μm. (H) Quantification of

fibrin-positive areas in tumor sections stained with anti-fibrin Ab. Data are means ± SEM, n=8 and are representative of 3 independent experiments including 8 mice per group.

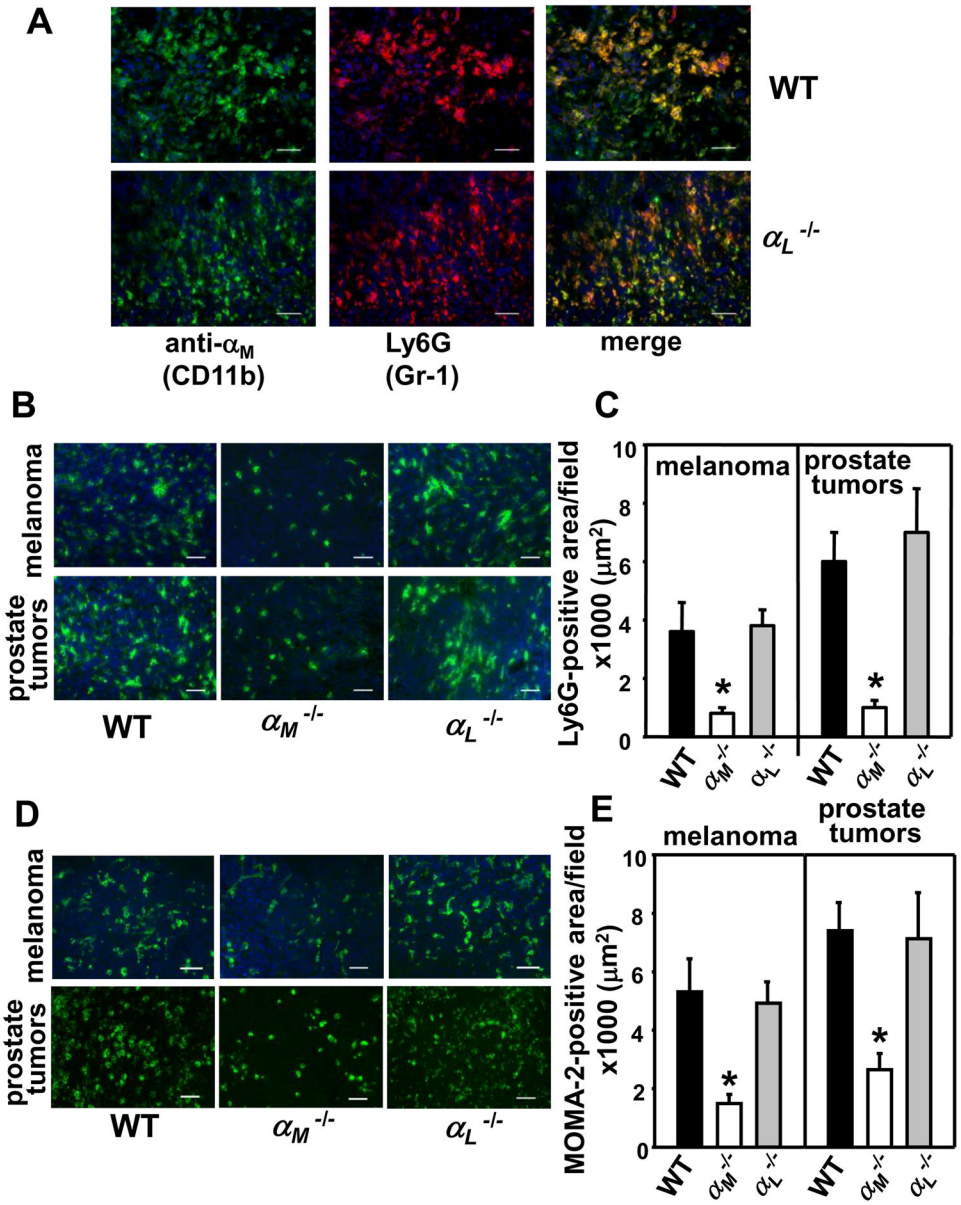

FIGURE 3.

Reduced leukocyte infiltration of tumors in the $\alpha_M^{-/-}$ mice. (A) Prostate tumor sections from WT and $\alpha_L^{-/-}$ mice were double stained with FITC-labeled rat anti-CD11b (M1/70) mAb (green) and rat anti-Ly6G (Gr-1) (clone 1A8-red). Numerous $CD11b^+/Gr\text{-}1^+$ cells are present on merged images (yellow/orange) in both mouse strains. Scale bars, 50 μm. Representative images of the melanoma and prostate tumor sections stained with PMN-specific anti-Ly6G (B) and the monocyte/macrophage-specific MOMA-2 (D) antibodies, Scale bar, 50 μm. (C&E) Image analysis shows reduced Ly6G-positive (C) and MOMA-2-positive (E) area in melanoma and prostate tumors in the $\alpha_M^{-/-}$ mice. Data are means ± SEM, (n=8 mice per group) and are representative of 3 independent experiments.

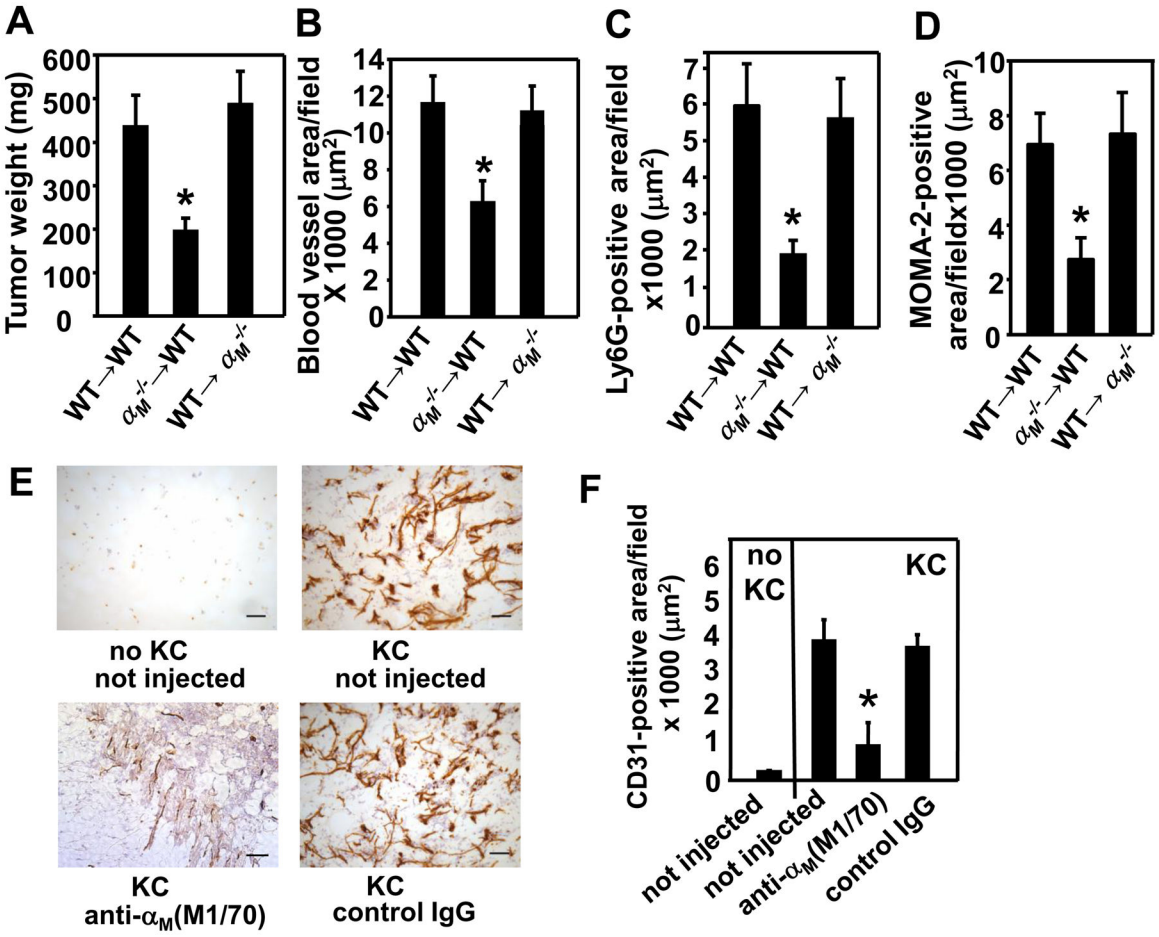

FIGURE 4.

Defective hematopoietic cells contribute to reduced tumor growth and angiogenesis in the $\alpha_M^{-/-}$ mice. (A) Average weight and (B) CD31-positive vascular area in RM1 prostate tumors in mice undergoing BMT with WT or $\alpha_M^{-/-}$ donor marrow. Data represent mean ± SEM, (n=5 mice per group) (C) Ly6G-positive and monocyte/macrophage-positive (D) area in RM1 tumors in mice undergoing BMT with WT or $\alpha_M^{-/-}$ donor marrow. Data represent mean ± SEM, (n=5 mice per group) (E&F) Intravenous administration of blocking mAb (M1/70) to $\alpha_M^{-/-}$ inhibits KC-dependent angiogenesis in Matrigel plug model in WT mice. M1/70 and normal rat IgG_{2b} (3.5 mg/kg) were injected before Matrigel injection and on days 2, 4 and 6. Matrigel implants were harvested on day 8, sectioned and stained with anti-CD31 mAb. (E) Representative images of Matrigel sections stained with anti-CD31 (brown), Scale bars, 50 μm (F) Quantification of the CD31-positive area in Matrigel implants. Data are means ± SEM, n=4 and are representative of 2 independent experiments.

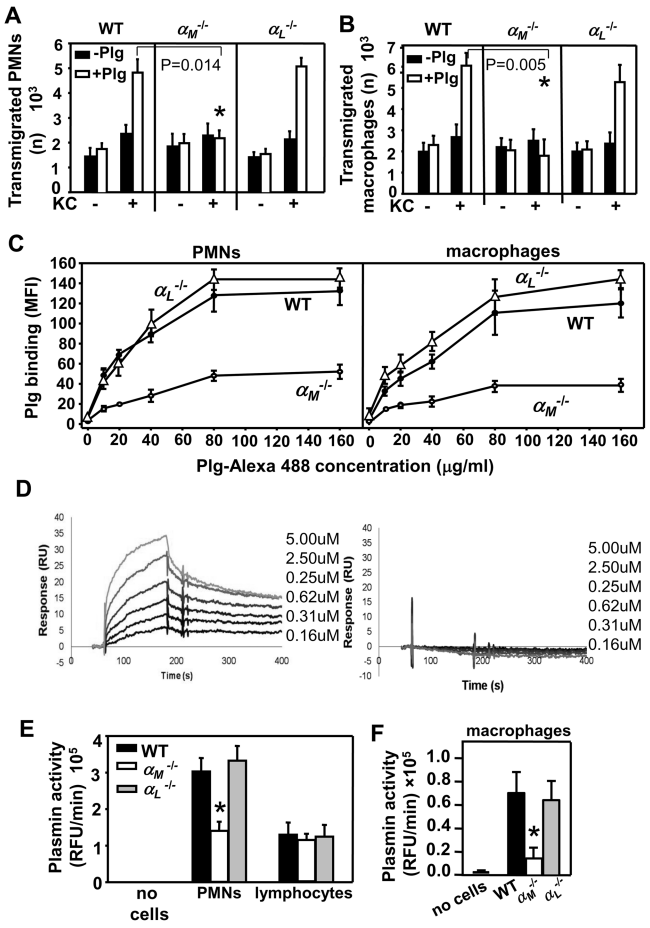

FIGURE 5.

$\alpha_M\beta_2$ directly interacts with Plg, enhances its activation and facilitates Plm-dependent leukocyte recruitment. KC-directed transmigration of peritoneal PMNs (A) and macrophages (B) through Matrigel-coated inserts is Plg-dependent and is impaired in $\alpha_M^{-/-}$ leukocytes. The data are means ± SEM of triplicate samples and are representative of two independent experiments including 3 mice per group. (C) Reduced binding of soluble Alexa488-labeled Plg to peritoneal $\alpha_M^{-/-}$ PMNs and macrophages. The cells were incubated with increasing concentrations of Plg as indicated for 30 min at 37°C. After two washings, Plg binding to cell surface was analyzed using a FACSCalibur flow cytometer and CellQuest software. The cells incubated without Plg were set as negative controls. The data are means ± SEM of triplicate samples, 3 mice per group and are representative of two independent experiments. (D) Plg was immobilized on the CM5 sensor chip surfaces (500 RU). Sensograms obtained for a concentration series of GST-α_M-I (left panel) and GST-α_L–I domain (right panel). (E&F) Reduced Plg activation on the surface of peripheral blood $\alpha_M^{-/-}$ PMNs and peritoneal macrophages. The results are means ± SEM of triplicate samples, n=5 mice per group and are representative of two independent experiments.

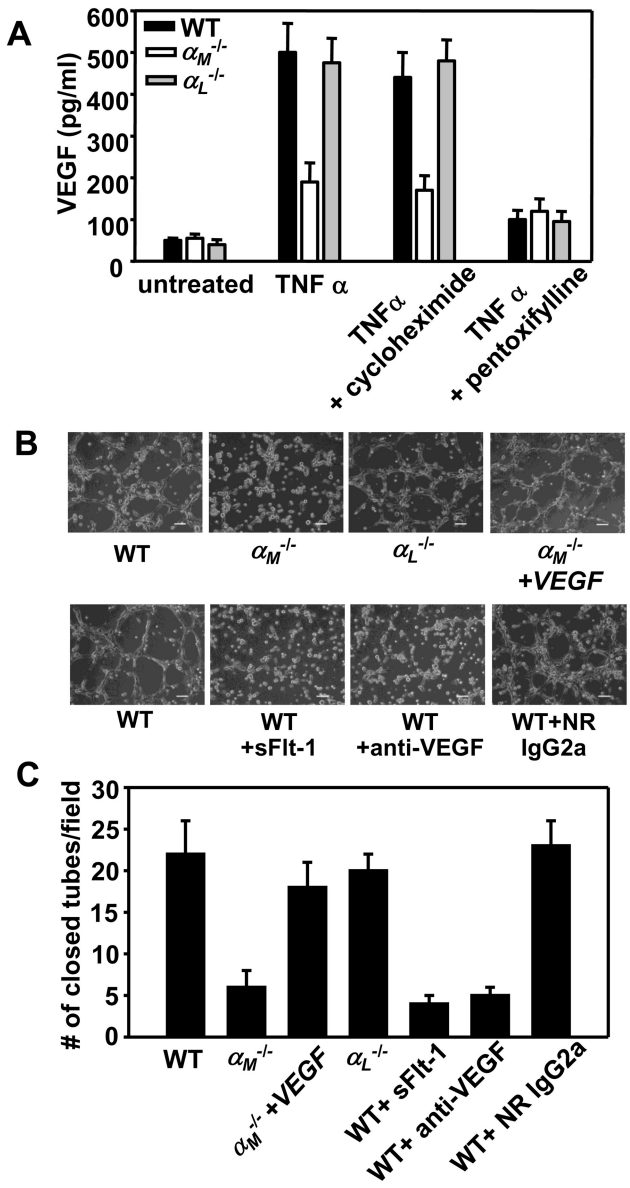

FIGURE 6.

$\alpha_M\beta_2$ supports angiogenesis via regulation of VEGF secretion by PMNs. (A) Peripheral blood WT, $\alpha_M^{-/-}$ or $\alpha_L^{-/-}$ PMNs (3×10^6 cells/well) were incubated in 24-well TC plates in the absence or presence of TNFα (20ng/ml) for 2h at 37°C. Cycloheximide (10μg/ml) or pentoxifylline (300 μM) were added 60 min before addition of TNFα. VEGF concentration was measured in supernatants using mouse VEGF Quantikine Elisa Kit. Data are means ± SEM of triplicate samples and are representative of three independent experiments. (B) Bright field microscopy of tube formation by WT MAECs in the presence of conditioned media collected from WT, $\alpha_M^{-/-}$ or $\alpha_L^{-/-}$ peripheral blood PMNs stimulated with TNFα (upper panels). Inhibitors of VEGF: neutralizing anti-VEGF mAb, isotype matched rat IgG_{2a} (100 μg/ml) and recombinant mouse sFLT-1 (100ng/ml) were preincubated for 60 min with conditioned media of WT TNFα-stimulated PMNs before its addition to MAECs

(lower panels). The images were taken after 6h incubation in 37°C, 5% CO_2. Scale bars, 75 μm. (C) Quantification of tube formation. Number of closed tubes was counted in 20 different fields of each treatment and plotted as mean ± SEM and are representative of two independent experiments.

Table 1

Comparison of VEGF-A mRNA content in WT, $\alpha_M^{-/-}$ and $\alpha_L^{-/-}$ peripheral blood PMNs. Values are expressed relative to GAPDH mRNA levels

Treatment	WT	$\alpha_M^{-/-}$	$\alpha_L^{-/-}$
Untreated	0.22	0.19	0.2
TNFα (20 ng/ml)	0.24	0.20	0.24

PMNs were incubated in the presence or absence of TNFα (20 ng/ml) for 2h at 37°C, total RNA was isolated using Trizol reagent and RT-PCR has been performed as described in Materials and Methods.